ERDC/CRREL M-05-1

Cold Regions Research and Engineering Laboratory

US Army Corps of Engineers®
Engineer Research and Development Center

Handbook of Physical Constants and Functions for Use in Atmospheric Boundary Layer Studies

Edgar L Andreas

October 2005

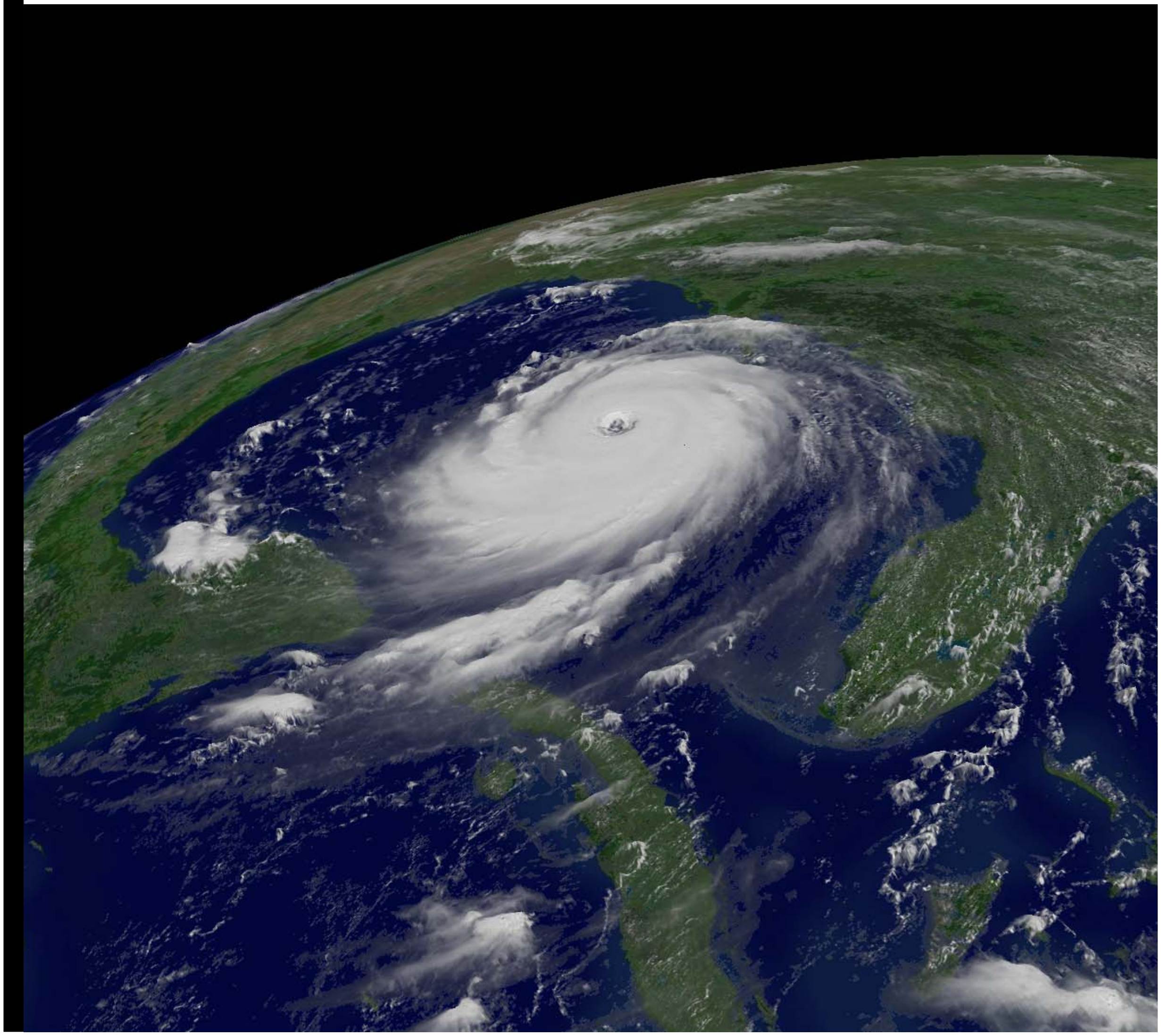

Cover: Hurricane Katrina as a category 5 storm in the Gulf of Mexico at 1515 UT on 28 August 2005. GOES-12 visible image courtesy of the National Oceanic and Atmospheric Administration.

ERDC/CRREL M-05-1
October 2005

Handbook of Physical Constants and Functions for Use in Atmospheric Boundary Layer Studies

Edgar L Andreas

Cold Regions Research and Engineering Laboratory
U.S. Army Engineer Research and Development Center
72 Lyme Road
Hanover, New Hampshire 03755

Prepared for Department of the Army
Office of Naval Research

ABSTRACT

Studies of the atmospheric boundary layer always require values for the dynamic and thermodynamic properties of the fluids present: namely, air, water vapor, and other trace gases. Studies of the marine boundary layer frequently require similar properties for the ocean, in addition. This handbook collects functions for calculating the values for these dynamic and thermodynamic variables. For example, it includes equations for air density, water vapor density, and seawater density. It also describes various humidity variables and shows how to convert among these. It includes equations for the specific heats of dry air, water vapor, moist air, seawater, and ice and for the latent heats of water in its various phases. The handbook goes on to show how to calculate the molecular transport properties such as the thermal conductivity of air and the diffusivities of heat, water vapor, and several environmentally important gases in air. This discussion naturally includes values for the molecular Prandtl and Schmidt numbers. Finally, the handbook concludes with summaries of several wind force scales that descriptively categorize winds on land and sea: the Beaufort Scale, the Saffir-Simpson Scale for hurricanes, and the Fujita Scale for tornadoes.

CONTENTS

ILLUSTRATIONS

TABLES

LIST OF SYMBOLS

B	Beaufort number or force [see (14.1)]
c_p	Specific heat of air at constant pressure
$\tilde{c}_p$	General value of the specific heat of air at constant pressure [see (6.3)]
c_{pd}	Specific heat of dry air at constant pressure [see (6.1)]
c_{pi}	Specific heat of pure ice at constant pressure [see (6.10)]
c_{ps}	Specific heat of seawater at constant pressure [see (6.8)]
c_{pv}	Specific heat of water vapor at constant pressure [see (6.2)]
c_{pw}	Specific heat of pure water at constant pressure [see (6.9)]
D	Thermal diffusivity of air [see (11.2)]
D'	Thermal diffusivity of air modified for the effects of surface curvature [see (13.2)]
d_a	Effective diameter of an air molecule ($= 3.7 \times 10^{-10}$ m)
D_g	Diffusivity of an arbitrary gas in air [see (12.4)]
D_{gT}	Diffusivity of an arbitrary gas in air at a specified temperature and at pressure P_0 [see Table 5]
D_{g0}	Diffusivity of an arbitrary gas in air at temperature T_0 and pressure P_0 [see Table 5]
d_w	Diameter of a water molecule ($= 1.65 \times 10^{-10}$ m)
D_v	Molecular diffusivity of water vapor in air [see (12.1)]
D'_v	Molecular diffusivity of water vapor in air modified for the effects of surface curvature [see (13.3)]
e	Water vapor pressure
e_{sat}	Saturation pressure of water vapor [see (4.1)–(4.4)]
f	Fractional relative humidity (= RH/100)
F	Fujita number [see (14.2)]
H_s	Sensible heat flux [see (6.3)]
$H_{1/3}$	Significant wave height [see Table 6]
k	Boltzmann constant ($= 1.38065 \times 10^{-23}$ J K^{-1})

k_a	Thermal conductivity of air [see (11.1)]
k'_a	Thermal conductivity of air modified for the effects of surface curvature [see (13.1)]
L_f	Latent heat of fusion of water [see (7.2)]
L_s	Latent heat of sublimation of ice [see (7.3)]
L_v	Latent heat of vaporization of water [see (7.1)]
M_a	Molecular weight of air (= 28.9644×10^{-3} kg mol^{-1})
m_s	Mass of salt in a seawater sample
m_w	Mass of pure water in a seawater sample
M_w	Molecular weight of water (= 18.015×10^{-3} kg mol^{-1})
P	Barometric pressure
P_0	Standard pressure; i.e., one atmosphere (= 1013.25 mb)
Pr	Molecular Prandtl number [see (12.2)]
Q	Specific humidity [see (4.6)]
Q_{sat}	Saturation specific humidity [see (4.7)]
r	Mixing ratio [see (4.9)]
R	Universal gas constant (= 8.31447 J mol^{-1} K^{-1})
RH	Relative humidity in percent [see (4.12) and (4.15)]
r_{sat}	Saturation mixing ratio [see (4.10)]
r_0	Radius of an atmospheric aerosol
s	Fractional salinity [see (8.3)] (= S/1000)
S	Salinity in practical salinity units (psu)
Sc	Molecular Schmidt number [see (12.3)]
t	Turbulent fluctuation in temperature [see (6.3)]
T	Temperature
T_a	Air temperature
T_d	Dew-point or frost-point temperature
T_f	Freezing point of seawater [see (5.3)]
T_v	Virtual temperature [see (3.8)]

T_{wet}	Wet-bulb temperature
T_0	Standard temperature (= 273.15 K)
U	Surface-level wind speed [see (14.2)]
U_{10}	Wind speed at a height of 10 m [see (14.1)]
w	Turbulent fluctuation in vertical velocity [see (6.3)]
α_c	Empirical constant in the equation for the modified water vapor diffusivity [see (13.3)] (= 0.036)
α_T	Empirical constant in the equation for the modified thermal conductivity [see (13.1)] (= 0.7)
Δ_T	Empirical length scale in the equation for the modified thermal conductivity [see (13.1)] (= 2.16×10^{-7} m)
Δ_v	Empirical length scale related to the mean free path of an air molecule and used in the equation for the modified water vapor diffusivity [see (13.3)] (= 8.7×10^{-8} m)
η_a	Dynamic viscosity of air [see (10.1)]
η_w	Dynamic viscosity of pure water [see (10.4)]
λ_a	Mean free path of air molecules [see (9.4)]
λ_v	Mean free path of water vapor molecules in air [see (9.5)]
ν_a	Kinematic viscosity of air [see (10.3)]
ν_{sw}	Kinematic viscosity of seawater [see (10.6)]
ν_w	Kinematic viscosity of pure water [see (10.5)]
ρ_a	Density of moist air [see (3.5) and (3.7)]
$\tilde{\rho}_a$	Air density in general [see (6.3)]
ρ_d	Density of dry air [see (2.2) and (3.2)]
ρ_{d0}	Density of dry air at standard temperature and pressure [see (2.2)] (= 1.2922 kg m^{-3})
ρ_{sw}	Density of seawater [see (5.2)]
ρ_v	Density of water vapor (or absolute humidity) [see (3.1)]
$\rho_{v,sat}$	Saturation water vapor density
ρ_w	Density of pure water [see (5.1) and (5.5)]

σ_{sw}	Surface tension of an interface between water vapor and seawater [see (8.5)]
σ_{w}	Surface tension of an interface between water vapor and pure water [see (8.1) and (8.2)]

PREFACE

This report was prepared by Dr. Edgar L Andreas, Research Physicist, Snow and Ice Branch, U.S. Army Cold Regions Research and Engineering Laboratory (CRREL), Engineer Research and Development Center (ERDC), Hanover, New Hampshire.

Funding was provided by the Department of the Army through Project 611102T2400 and by the Office of Naval Research through award N0001405MP20044. Dr. Andreas thanks Gary Koh, Janet P. Hardy, and Dr. Charles C. Ryerson for reviewing the manuscript. He also thanks Dr. E. Frank Bradley of the Commonwealth Scientific and Industrial Research Organization and Dr. Christopher W. Fairall of NOAA's Environmental Technology Laboratory for encouraging him to prepare this material.

This report was prepared under the general supervision of Dr. Charles C. Ryerson, Chief, Snow and Ice Branch; Dr. Lance Hansen, Deputy Director; and James L. Wuebben, Acting Director, CRREL.

The Commander and Executive Director of the Engineer Research and Development Center is COL James R. Rowan. The Director is Dr. James R. Houston.

Handbook of Physical Constants and Functions for Use in Atmospheric Boundary Layer Studies

EDGAR L ANDREAS

1 INTRODUCTION

Studies of geophysical boundary layers always require kinematic and thermodynamic constants for the fluids involved. The most obvious examples are for the fluid densities: air, pure water, seawater, and water vapor. Boundary-layer studies frequently involve exchanging properties across interfaces; consequently, molecular properties like the kinematic viscosity, thermal conductivity, water vapor diffusivity, and surface tension are also necessary. In turn, the ratios of the molecular transport quantities—the Prandtl and Schmidt numbers—are recurring variables.

Here, I summarize the values and functions for these and other quantities that I have found to be accurate and useful for my work in boundary-layer meteorology. This handbook is admittedly not all-encompassing. For example, I tend to focus on the quantities and the range of conditions for studies of air–land, air–sea, and air–sea–ice interaction. I also describe some microphysical quantities used in studies of aqueous solution droplets, like cloud droplets and sea spray. I tend to simply describe ways to calculate the quantities of interest without also explaining why you might want this quantity. Therefore, check any good book on atmospheric thermodynamics, such as Iribarne and Godson (1981), Pruppacher and Klett (1997), or Bohren and Albrecht (1998), for academic discussions of the thermodynamic quantities.

2 AIR DENSITY

Dry air obeys the ideal gas law,

$$\rho_d = \frac{M_a P}{R T} , \tag{2.1}$$

where ρ_d = density of dry air

M_a = molecular weight of air

P = barometric pressure

R = universal gas constant

T = air temperature (K).

At standard temperature ($T = T_0 = 273.15$ K) and pressure ($P = P_0 = 1013.25$ mb), (2.1) gives $\rho_{d0} = 1.2922$ kg m^{-3}. Therefore, (2.1) also gives

$$\rho_d = \rho_{d0} \left(\frac{T_0}{T} \right) \left(\frac{P}{P_0} \right) = 1.2922 \left(\frac{T_0}{T} \right) \left(\frac{P}{P_0} \right) , \tag{2.2}$$

where ρ_d is in kg m^{-3} when P is in millibars and T is in kelvins.

3 WATER VAPOR DENSITY

Water vapor in the atmosphere also obeys the ideal gas law,

$$\rho_v = \frac{M_w e}{R T} , \tag{3.1}$$

where ρ_v = water vapor density

M_w = molecular weight of water

e = partial pressure of the water vapor.

To be rigorous, we need to recognize that, in (2.1), the partial pressure of dry air is not the barometric pressure P but rather is approximately P – e. That is, in rigorous usage, (2.1) should be

$$\rho_d = \frac{M_a \left(P - e\right)}{R T} . \tag{3.2}$$

By rearranging (3.1) and (3.2), we can write the following expression for the barometric pressure:

$$P = \left(P - e\right) + e = \frac{R T \rho_d}{M_a} + \frac{R T \rho_v}{M_w} , \tag{3.3}$$

or

$$P = \frac{R T \rho_a}{M_a}\left[1 + \left(\frac{M_a}{M_w} - 1\right)\frac{\rho_v}{\rho_a}\right] . \tag{3.4}$$

Here,

$$\rho_a = \rho_d + \rho_v \tag{3.5}$$

is the density of moist air; and we recognize ρ_v/ρ_a as the specific humidity, Q (more on this soon).

Equation (3.4) rearranges to

$$\rho_a = \frac{M_a P}{R T (1 + 0.608 Q)} , \tag{3.6}$$

where $M_a/M_w - 1 = 0.608$. Equation (3.6) implies that (2.1) is inaccurate by the factor $(1 + 0.608Q)$ if we want the total air density. Since for normal atmospheric conditions Q is seldom larger than 0.035 kg kg^{-1}, the term in parentheses in (3.6) is always between 1.000 and 1.022. Therefore, (2.1) may be accurate enough for many purposes.

Nevertheless, we often rewrite (3.6) as (e.g., Lumley and Panofsky 1964, p. 214)

$$\rho_a = \frac{M_a P}{R T_v} \tag{3.7}$$

to preserve the form of (2.1) while retaining the accuracy of (3.6) by defining the virtual temperature

$$T_v = T (1 + 0.608 Q) . \tag{3.8}$$

In effect, T_v is the temperature that dry air must have to produce the same density as moist air at the given barometric pressure.

4 WATER VAPOR VARIABLES

Many types of instruments are available for measuring atmospheric water vapor. Some actually measure the water vapor density (the absolute humidity), but many measure derivative quantities such as the mixing ratio, the dew-point temperature, or the wet-bulb temperature. Hence, analyses and data reporting often require converting among the different water vapor variables. Schwerdtfeger (1976) and Pruppacher and Klett (1997, p. 106f.), among many others, give good summaries of water vapor variables.

4.1 Vapor Pressure

If there is a fundamental water vapor quantity, I'd say it is the vapor pressure e. And for computational purposes, the saturation vapor pressure e_{sat} is usually the fundamental variable.

I use Buck's (1981) three equations for the saturation vapor pressure (cf. Brock and Richardson 2001, p. 86ff.). For vapor in saturation with a planar surface of pure water at temperature T between –20° and 50°C, Buck gives

$$e_{sat}(T) = 6.1121\left(1.0007 + 3.46\times10^{-6}\,P\right)\exp\left(\frac{17.502\,T}{240.97+T}\right), \tag{4.1}$$

where e_{sat} is in millibars when P, the barometric pressure, is also in millibars.

For saturation over water at much lower temperatures, $-40° \le T \le 0°C$, Buck (1981) gives

$$e_{sat}(T) = 6.1121\left(1.0007 + 3.46\times10^{-6}\,P\right)\exp\left(\frac{17.966\,T}{247.15+T}\right). \tag{4.2}$$

Use this relation, for example, to compute the saturation vapor pressure in clouds composed of deeply supercooled water droplets.

Finally, if the vapor is in equilibrium with a surface of pure ice (or snow, for instance), Buck (1981) recommends the following equation for $-50° \le T \le 0°C$:

$$e_{sat}(T) = 6.1115\left(1.0003 + 4.18\times10^{-6}\,P\right)\exp\left(\frac{22.452\,T}{272.55+T}\right). \tag{4.3}$$

As an alternative for the saturation vapor pressure over ice, Murphy and Koop (2005) give a more complex expression that extends over a wider temperature range, –165.15° ≤ T ≤ 0°C;

$$e_{sat}(T) = 0.01\left[1 + 10^{-5} P\left(4.923 - 0.0325T + 5.84\times10^{-5} T^{2}\right)\right] \bullet \exp\left[9.550426 - \frac{5723.265}{T} + 3.53068\ln(T) - 0.00728332T\right] . \quad (4.4)$$

This gives e_{sat} in millibars for P in millibars and T in kelvins. Equations (4.3) and (4.4) differ insignificantly over their common range. I therefore prefer (4.3) because it is mathematically simpler. Use (4.4), however, for temperatures below –50°C.

Figure 1 shows e_{sat} as a function of temperature for saturation over water, over supercooled water, and over ice. Instruments that measure the dew-point or frost-point temperature essentially provide the temperature T in (4.1)–(4.4). Hence, Figure 1 is equivalently a plot of saturation vapor pressure versus dew-point or frost-point temperature, depending on whether the surface in equilibrium is water or ice.

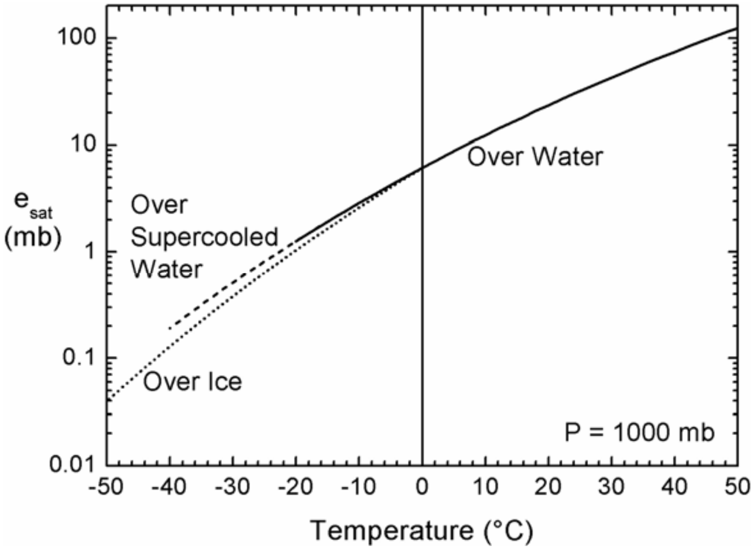

Figure 1. Saturation vapor pressure as a function of temperature for three regimes: vapor over a water surface [i.e., (4.1)], vapor over supercooled water [i.e., (4.2)], and vapor over ice [i.e., (4.3)]. The barometric pressure is assumed to be 1000 mb.

When the water surface is not pure but, for example, is seawater with salinity S, the saturation vapor pressure is depressed to $e_{sat}(T,S)$, where (e.g., Roll 1965, p. 262; List 1984, p. 373)

$$\frac{e_{sat}(T,S)}{e_{sat}(T)} = 1 - 0.000537S \ . \qquad (4.5)$$

Here, the salinity is in psu. Equation (4.5) means that, for a typical open-ocean salinity of 35 psu, water vapor in saturation with the surface has a vapor pressure that is 98.1% of the vapor pressure over a pure water surface with the same temperature.

The discussion naturally turns now to how to treat a sea ice surface. The point is often moot, however, because sea ice is usually snow covered, so we would just compute the saturation vapor pressure as that for pure ice using (4.3) or (4.4). If the surface is truly bare sea ice, on the other hand, such as for new ice in a freezing lead or summer sea ice when the snow has all melted, we could still reasonably just use the saturation vapor pressure relation for pure ice. Freezing seawater rejects salt; consequently, sea ice rarely has a surface salinity above 8 psu. If we assume that (4.5) is also appropriate for sea ice—a reasonable assumption—the depression in vapor pressure over sea ice with salinity 8 psu would be only about 0.4%. Most humidity sensors cannot resolve such small changes in vapor pressure. Nevertheless, if such differences are important, (4.5) should be adequate for quantifying them.

4.2 Specific Humidity

Most other water vapor variables are calculated from the actual vapor pressure e and the saturation vapor pressure e_{sat}. For example, (3.1) shows how to compute the water vapor density ρ_v from the vapor pressure. The saturation vapor density $\rho_{v,sat}$ likewise comes from (3.1) with e_{sat} substituted for e.

The specific humidity is defined as

$$Q = \frac{\rho_v}{\rho_d + \rho_v} \ , \qquad (4.6)$$

and the saturation specific humidity is

$$Q_{sat} = \frac{\rho_{v,sat}}{\rho_d + \rho_{v,sat}} \ . \qquad (4.7)$$

Notice that, from (3.1) and (3.2),

$$Q = \frac{M_w e}{M_a (P-e) + M_w e} = \frac{\frac{M_w}{M_a}\frac{e}{P}}{1-\left(1-\frac{M_w}{M_a}\right)\frac{e}{P}} = \frac{0.622(e/P)}{1-0.378(e/P)} \ . \qquad (4.8)$$

That is, the specific humidity also derives from the vapor pressure. In SI units, specific humidity is given in kg kg^{-1}.

4.3 Mixing Ratio

The mixing ratio is defined as

$$r = \frac{\rho_v}{\rho_d} \ , \qquad (4.9)$$

and the saturation mixing ratio is

$$r_{sat} = \frac{\rho_{v,sat}}{\rho_d} \ . \qquad (4.10)$$

As with (4.8), we can also write r in terms of the vapor pressure. From (3.1) and (3.2),

$$r = \frac{M_w e}{M_a (P-e)} = \frac{\frac{M_w}{M_a}\frac{e}{P}}{1-\frac{e}{P}} = \frac{0.622(e/P)}{1-(e/P)} \ . \qquad (4.11)$$

4.4 Relative Humidity

Officially, the relative humidity (in percent) is defined as the ratio of mixing ratios (Bohren and Albrecht 1998, p. 198; Glickman 2000, p. 642f.),

$$RH = 100\left(\frac{r}{r_{sat}}\right) \ . \qquad (4.12)$$

From the definitions of mixing ratios, though, we see that

$$RH = 100\left(\frac{e}{P-e}\right)\left(\frac{P-e_{sat}}{e_{sat}}\right) . \tag{4.13}$$

We can rearrange this as

$$\begin{aligned} RH &= 100\left(\frac{e}{e_{sat}}\right)\left[\frac{1-(e_{sat}/P)}{1-(e/P)}\right] \\ &\simeq 100\left(\frac{e}{e_{sat}}\right)\left[1-\left(\frac{e_{sat}-e}{P}\right)-\frac{e_{sat}\,e}{P^2}\right] \end{aligned} . \tag{4.14}$$

Over marine surfaces, for example, e_{sat}/P and e/P are usually less than 0.03, and e is rarely less than 0.5 e_{sat}. Hence, for practical purposes, we can generally ignore the term in square brackets in (4.14); (4.12) is, thus, equivalent to the traditional definition of relative humidity,

$$RH = 100\left(\frac{e}{e_{sat}}\right) . \tag{4.15}$$

Furthermore, Bohren and Albrecht (1998, p. 186) prefer (4.15) to (4.12) because it better reflects the physics of evaporation and condensation processes. I likewise use (4.15) as my definition of relative humidity.

Table 1 shows the relative humidity as a function of air temperature and dew-point temperature, where I use (4.15) to define relative humidity.

4.5 Wet-Bulb Temperature

The wet-bulb temperature, T_{wet}, is another common humidity variable (e.g., Schwerdtfeger 1976, p 50ff.). A wetted thermometer will read lower than the ambient air temperature because of evaporation (but higher with condensation), and that rate of evaporation depends on the mixing ratio. At equilibrium, a well-ventilated wet-bulb thermometer obeys (Andreas 1995; Bohren and Albrecht 1998, p. 218ff)

$$c_p(T_a)(T_a - T_{wet}) = L_v(T_a)\left[r_{sat}(T_{wet}) - r\right] , \tag{4.16}$$

where c_p = specific heat of dry air at temperature T_a
L_v = latent heat of vaporization at T_a
r = ambient mixing ratio
r_{sat} = saturation mixing ratio at the wet-bulb temperature.

Rearranging (4.16) shows that the wet-bulb temperature predicts the mixing ratio,

$$r = r_{sat}\left(T_{wet}\right) - \frac{c_p\left(T_a\right)}{L_v\left(T_a\right)}\left(T_a - T_{wet}\right) \; . \qquad (4.17)$$

Table 1. Relative humidity (RH, in percent), from (4.15), as a function of the air temperature (T_a) and the dew-point depression, where T_d is the dew-point temperature (frost-point temperature for T_d less than 0°C). The barometric pressure P is assumed to be 1000 mb.

	Dew-Point Depression, $T_a - T_d$ (°C)													
T_a (°C)	**0.0**	**0.2**	**0.4**	**0.6**	**0.8**	**1.0**	**1.5**	**2.0**	**3.0**	**4.0**	**5.0**	**6.0**	**8.0**	**10.0**
–40	100	97.8	95.6	93.4	91.3	89.3	84.3	79.6	70.9	63.1	56.1	49.8	39.2	30.7
–35	100	97.9	95.7	93.7	91.7	89.7	84.9	80.4	71.9	64.3	57.5	51.3	40.7	32.2
–30	100	97.9	95.9	93.9	92.0	90.1	85.5	81.1	72.9	65.5	58.8	52.7	42.3	33.8
–25	100	98.0	96.1	94.2	92.3	90.5	86.0	81.8	73.8	66.6	60.1	54.1	43.8	35.3
–20	100	98.1	96.2	94.4	92.6	90.8	86.5	82.4	74.7	67.7	61.3	55.5	45.3	36.8
–15	100	98.2	96.4	94.6	92.9	91.2	87.0	83.0	75.6	68.7	62.5	56.7	46.7	38.3
–10	100	98.2	96.5	94.8	93.1	91.5	87.5	83.6	76.4	69.7	63.6	58.0	48.1	39.7
–5	100	98.3	96.6	95.0	93.4	91.8	87.9	84.2	77.2	70.7	64.7	59.2	49.4	41.1
0	100	98.4	96.8	95.2	93.6	92.1	88.3	84.7	77.9	71.6	65.7	60.3	50.7	42.5
5	100	98.6	97.2	95.9	94.6	93.2	90.0	86.9	80.9	75.3	70.1	64.5	54.6	46.1
10	100	98.7	97.4	96.1	94.8	93.5	90.4	87.4	81.6	76.2	71.1	66.3	57.5	49.8
15	100	98.7	97.5	96.2	95.0	93.7	90.7	87.8	82.3	77.0	72.0	67.3	58.8	51.2
20	100	98.8	97.5	96.3	95.2	94.0	91.1	88.3	82.9	77.8	72.9	68.4	60.0	52.5
25	100	98.8	97.6	96.5	95.3	94.2	91.4	88.7	83.5	78.5	73.8	69.4	61.2	53.8
30	100	98.9	97.7	96.6	95.5	94.4	91.7	89.1	84.0	79.2	74.6	70.3	62.3	55.1
35	100	98.9	97.8	96.7	95.7	94.6	92.0	89.4	84.5	79.9	75.4	71.2	63.4	56.3
40	100	98.9	97.9	96.8	95.8	94.8	92.3	89.8	85.0	80.5	76.2	72.1	64.4	57.5

And in light of (4.11),

$$e = e_{sat}\left(T_{wet}\right)\left(\frac{P - e}{P - e_{sat}}\right) - \frac{M_a}{M_w}\frac{\left(P - e\right)c_p\left(T_a\right)}{L_v\left(T_a\right)}\left(T_a - T_{wet}\right) , \tag{4.18}$$

which is approximately

$$e \simeq e_{sat}\left(T_{wet}\right) - \frac{P\,c_p\left(T_a\right)}{0.622\,L_v\left(T_a\right)}\left(T_a - T_{wet}\right) . \tag{4.19}$$

That is, the wet-bulb temperature also predicts the vapor pressure. Table 2 shows the vapor pressure computed from (4.19) for a range of T_a and $T_a - T_{wet}$ values.

Equations (4.17) and (4.19) apply to perfect wet-bulb thermometers. Schwerdtfeger (1976, p. 51f.) and Brock and Richardson (2001, p. 94) describe some second-order corrections that may be necessary to account for ventilation rate, radiative effects, and the size of the wet bulb.

Table 2. Vapor pressure (e, in mb) from (4.19) as a function of the air temperature (T_a) and the wet-bulb depression for wet-bulb temperatures above freezing. The column with $T_a - T_{wet} = 0$ is also the saturation vapor pressure (e_{sat}) at the indicated air temperature; consequently, the ratio of e at $T_a - T_{wet} > 0$ to e_{sat} is the fractional relative humidity (f) at $T_a - T_{wet}$. The barometric pressure P is assumed to be 1000 mb.

	Wet-Bulb Depression, $T_a - T_{wet}$ (°C)													
T_a (°C)	**0.0**	**0.2**	**0.4**	**0.6**	**0.8**	**1.0**	**1.5**	**2.0**	**3.0**	**4.0**	**5.0**	**6.0**	**8.0**	**10.0**
0	6.1													
2	7.1	6.9	6.6	6.4	6.2	6.0	5.4	4.8						
4	8.2	7.9	7.7	7.4	7.2	7.0	6.4	5.8	4.7	3.5				
6	9.4	9.1	8.9	8.6	8.4	8.1	7.5	6.9	5.7	4.5	3.3	2.2		
8	10.8	10.5	10.2	9.9	9.7	9.4	8.7	8.1	6.8	5.6	4.4	3.2	0.9	
10	12.3	12.0	11.7	11.4	11.2	10.9	10.2	9.5	8.1	6.8	5.5	4.3	1.9	
12	14.1	13.8	13.5	13.1	12.8	12.5	11.8	11.0	9.6	8.2	6.8	5.5	2.9	0.5
14	16.0	15.7	15.4	15.0	14.7	14.4	13.6	12.8	11.2	9.7	8.2	6.8	4.1	1.6
16	18.3	17.9	17.5	17.2	16.8	16.5	15.6	14.7	13.1	11.5	9.9	8.4	5.5	2.8
18	20.7	20.3	19.9	19.6	19.2	18.8	17.9	16.9	15.1	13.4	11.7	10.1	7.1	4.2
20	23.5	23.0	22.6	22.2	21.8	21.4	20.4	19.4	17.5	15.6	13.8	12.1	8.8	5.7
22	26.5	26.1	25.6	25.2	24.7	24.3	23.2	22.1	20.1	18.1	16.1	14.3	10.8	7.5
24	30.0	29.5	29.0	28.5	28.0	27.5	26.4	25.2	23.0	20.8	18.7	16.7	13.0	9.4
26	33.7	33.2	32.7	32.2	31.7	31.1	29.9	28.6	26.2	23.9	21.6	19.5	15.4	11.6
28	38.0	37.4	36.8	36.2	35.7	35.1	33.8	32.4	29.8	27.3	24.9	22.6	18.2	14.1
30	42.6	42.0	41.4	40.8	40.2	39.6	38.1	36.6	33.8	31.1	28.5	26.0	21.2	16.8
32	47.8	47.1	46.4	45.8	45.1	44.5	42.9	41.3	38.2	35.3	32.5	29.7	24.6	19.9
34	53.4	52.7	52.0	51.3	50.6	49.9	48.1	46.4	43.1	39.9	36.9	33.9	28.4	23.3
36	59.7	58.9	58.1	57.4	56.6	55.8	53.9	52.1	48.5	45.1	41.8	38.6	32.6	27.1
38	66.6	65.7	64.9	64.0	63.2	62.4	60.4	58.4	54.5	50.8	47.2	43.7	37.2	31.2
40	74.1	73.2	72.3	71.4	70.5	69.6	67.4	65.2	61.0	57.0	53.1	49.4	42.4	35.9

5 WATER DENSITY

I have found several modern expressions in the literature for the density of pure water, ρ_w. Any one would probably be accurate enough for the purposes of this handbook. This one is Gill's (1982, p. 599):

$$\begin{aligned}\rho_w &= 999.842594 + 6.793952\times10^{-2}\,T - 9.095290\times10^{-3}\,T^2 \\ &\quad + 1.001685\times10^{-4}\,T^3 - 1.120083\times10^{-6}\,T^4 + 6.536332\times10^{-9}\,T^5\end{aligned} \quad . \qquad (5.1)$$

It gives ρ_w in kg m^{-3} for a barometric pressure of one atmosphere when T is between 0° and 40°C.

To find the density of seawater, ρ_{sw}, with temperature T and salinity S for pressures near one atmosphere, Gill (1982, p. 599) gives

$$\begin{aligned}\rho_{sw} &= \rho_w + S(0.824439 - 4.0899\times10^{-3}\,T + 7.6438\times10^{-5}\,T^2 \\ &\quad - 8.2467\times10^{-7}\,T^3 + 5.3875\times10^{-9}\,T^4) \\ &\quad + S^{3/2}(-5.72466\times10^{-3} + 1.0227\times10^{-4}\,T - 1.6546\times10^{-6}\,T^2) \\ &\quad + 4.8314\times10^{-4}\,S^2\end{aligned} \quad . \qquad (5.2)$$

This is appropriate for S in [0, 42 psu] and T in [T_f, 40°C], where T_f is the freezing point of seawater with salinity greater than 0 psu.

Gill (1982, p. 602) gives T_f as a function of salinity for S between 0 and 40 psu; but I prefer Kester's (1974) formula, which is always within 0.01°C of Gill's for S in [1, 40 psu], because it is easier to invert. Kester gives T_f in °C as

$$T_f = -0.0137 - 5.1990\times10^{-2}\,S - 7.225\times10^{-5}\,S^2 \ . \qquad (5.3)$$

In turn, if we know that the seawater is at its freezing point, we can invert (5.3) to find the corresponding salinity,

$$\begin{aligned}S &= -3.598\times10^2 \\ &\quad + 6.920\times10^3\left[2.7030\times10^{-3} - 2.890\times10^{-4}\left(T_f + 0.0137\right)\right]^{1/2}\end{aligned} \ . \qquad (5.4)$$

For supercooled pure water in the temperature interval [–33°, 0°C], Pruppacher and Klett (1997, p. 87) give

$$\begin{aligned}\rho_w &= 999.86 + 6.690\times10^{-2}\,T - 8.486\times10^{-3}\,T^2 + 1.518\times10^{-4}\,T^3 \\ &\quad - 6.9984\times10^{-6}\,T^4 - 3.6449\times10^{-7}\,T^5 - 7.497\times10^{-9}\,T^6\end{aligned} \quad . \tag{5.5}$$

Here, again, ρ_w is in kg m^{-3} when T is in °C. Pruppacher and Klett have taken (5.5) directly from Hare and Sorensen (1987).

For completeness, I also include in this section an equation for the density of pure ice, ρ_i. Pruppacher and Klett (1997, p. 79f.) give

$$\rho_i = 916.7 - 0.175T - 5.0\times10^{-4}\,T^2 \ , \tag{5.6}$$

which yields ρ_i in kg m^{-3} for T in °C. Pruppacher and Klett claim that this relation fits the experimental data for T in [–180°, 0°C]. On comparing the predictions of (5.6) with Hobbs's (1974, p. 348) tabulation of ρ_i, I can further say that (5.6) is accurate to better than 0.5% over this range.

6 SPECIFIC HEAT

6.1 Specific Heat of Dry Air

The specific heat of air appears recurrently in studies of the atmospheric boundary layer. Using data from Hilsenrath et al. (1960), I have obtained the following polynomial prediction for the specific heat of dry air at constant pressure:

$$c_{pd} = 1005.60 + 0.017211T + 0.000392T^2 \ . \tag{6.1}$$

This gives c_{pd} in J kg^{-1} °C^{-1} for temperature T between –40° and 40°C and for barometric pressures near one atmosphere. Equation (6.1) has a minimum of 1005.41 J kg^{-1} °C^{-1} at –21.95°C.

6.2 Specific Heat of Water Vapor

Reid et al. (1987, p. 656f., 668) give a polynomial expression for the specific heat of water vapor at constant pressure for barometric pressures near one atmosphere. The temperature in their polynomial is in kelvins, however, and their units of c_{pv} are J mol^{-1} °C^{-1}. I have therefore converted their polynomial to

$$c_{pv} = 1858 + 3.820\times10^{-1}\,T + 4.220\times10^{-4}\,T^2 - 1.996\times10^{-7}\,T^3 \ , \tag{6.2}$$

which gives c_{pv} in J kg^{-1} °C^{-1} when T is in °C. Equation (6.2) should be accurate for all near-surface atmospheric temperatures.

6.3 In the Turbulent Sensible Heat Flux

A frequent use for the specific heat of air is in finding the turbulent sensible heat flux, which is defined as

$$H_s = \tilde{\rho}_a \, \tilde{c}_p \, \overline{wt} \ . \tag{6.3}$$

Here, w is the turbulent fluctuation in vertical wind velocity, t is the turbulent fluctuation in air temperature, and the overbar denotes a time average. The tildes over the ρ_a and the c_p terms in (6.3) denote these as general values of the air density and specific heat of air at constant pressure because confusion exists as to which values constitute the proper definition of sensible heat flux.

Most of the boundary-layer community simply use ρ_a, the density of moist air, for $\tilde{\rho}_a$ and c_{pd} for $\tilde{c}_p$. Businger's (1982) analysis confirms that this is proper practice for micrometeorological studies. That is, (6.3) would be

$$H_s = \rho_a c_{pd} \overline{wt} . \qquad (6.4)$$

On the other hand, when long time intervals or global averages define the scope of the study—for example, in balancing the hydrological cycle—Businger (1982) explains that the reference temperature for enthalpy transfer must be chosen carefully. When such "careful bookkeeping of the energy" is necessary, Businger concludes that the sensible heat flux must be expressed as

$$H_s = \left(\rho_d c_{pd} + \rho_v c_{pv}\right) \overline{wt} . \qquad (6.5)$$

Fuehrer and Friehe's [2002, Eq. (114)] extensive thermodynamic analysis yields essentially this same result, although they give it as general result—not one necessary only for large areal averages. They also include two other small terms in (6.5) that are associated with the flux of water vapor between temperature reference states.

As a practical exercise, I can check how different (6.4) and (6.5) are. We can convert (6.5) into a form similar to (6.4),

$$H_s = \rho_a c_{pd} \left[1 + Q\left(\frac{c_{pv} - c_{pd}}{c_{pd}}\right)\right] \overline{wt} . \qquad (6.6)$$

Using (6.1) and (6.2), we see that $(c_{pv} - c_{pd})/c_{pd}$ ranges from 0.861 to 0.833 for air temperatures between –40° and 40°C. Hence, I approximate (6.6) as (cf. Larsen and Busch 1974)

$$H_s \simeq \rho_a c_{pd} \left(1 + 0.85Q\right) \overline{wt} . \qquad (6.7)$$

As I mentioned earlier, Q is seldom larger than 0.035 kg kg^{-1} in the natural atmosphere, and it would attain this value, probably, only over the tropical ocean. Hence, (6.5) yields values of the sensible heat flux that are, at most, 3% larger than the values from (6.4). In many applications, this is a negligible difference, since $\overline{wt}$ usually is measured to no better than ±10%. And at temperatures below 0°C, where Q is less than 0.004 kg kg^{-1}, (6.4) and (6.5) differ by much less than 1%.

6.4 Specific Heat of Water

Both temperature and salinity influence the specific heat of seawater at constant pressure, c_{ps}. Neumann and Pierson (1966, p. 47) tabulate values of c_{ps} that come from data collected by Cox and Smith (1959). Horne (1969, p. 68) gives a functional expression for c_{ps} in terms of temperature and salinity that he converted from a similar expression that Bromley et al. (1967) deduced from their own measurements.

Millero et al. (1973) also reported measurements of c_{ps} and fitted an equation to these measurements in terms of temperature and chlorinity. Gill (1982, p. 601) converted this to an expression in terms of temperature and salinity. The following is essentially Gill's equation, although I have modified it slightly to better represent the precision that Millero et al. implied in their fitting coefficients:

$$\begin{aligned} c_{ps} = {} & c_{pw} + S\left(-7.6444 + 0.10728T - 1.384\times10^{-3}T^2\right) \\ & + S^{3/2}\left(0.177 - 4.08\times10^{-3}T + 5.35\times10^{-5}T^2\right) \end{aligned} . \tag{6.8}$$

Here, c_{pw} is the specific heat of pure water,

$$\begin{aligned} c_{pw} = {} & 4217.4 - 3.720283T + 0.1412855T^2 \\ & - 2.654387\times10^{-3}T^3 + 2.093236\times10^{-5}T^4 \end{aligned} . \tag{6.9}$$

In (6.8) and (6.9), T is in °C and ranges from T_f to 40°C; in (6.8), S is in psu and ranges from 0 to 40 psu. The pressure is assumed to be one atmosphere. Table 3 shows values of c_{ps} that result from (6.8).

The values in Table 3 are quite compatible with the values in Neumann and Pierson's (1966, p. 47) table, which are based on Cox and Smith's (1959) data. The values in Table 3, however, have some systematic differences from the results from Bromley et al. (1967; also Horne 1969, p. 67f.), especially for fresh water in the lower part of the temperature range. For example, Bromley et al. report $c_{pw} = 4207$ J kg^{-1} °C for T = 0°C, while Table 3 gives 4217 J kg^{-1} °C. Therefore, I conclude that (6.8) and (6.9) are accurate to roughly ±3 J kg^{-1} °C (cf. Bromley et al. 1967; Millero et al. 1973).

Table 3. Specific heat of seawater at constant pressure, c_{ps} (in J kg^{-1} °C^{-1}), as a function of temperature and salinity. These results come from (6.8). The barometric pressure is assumed to be one atmosphere.

		Salinity (psu)						
		0	**10**	**20**	**25**	**30**	**35**	**40**
Temperature (°C)	**0**	4217	4147	4080	4048	4017	3986	3956
	5	4202	4136	4073	4043	4014	3985	3956
	10	4192	4129	4070	4042	4014	3986	3959
	15	4186	4126	4070	4043	4016	3990	3964
	20	4182	4125	4071	4045	4019	3994	3969
	25	4179	4125	4072	4047	4022	3998	3974
	30	4178	4125	4074	4049	4025	4001	3977
	35	4178	4125	4075	4051	4027	4003	3980
	40	4178	4126	4076	4052	4028	4004	3981

6.5 Specific Heat of Ice

Murphy and Koop (2005) give a new expression for the specific heat of ice for temperatures down to 20 K. Because their units, however, are J mol^{-1} K^{-1}, I convert their expression to predict c_{pi} in J kg^{-1} K^{-1} using $M_w = 18.015 \times 10^{-3}$ kg mol^{-1}. The result is

$$c_{pi} = -114.19 + 8.1288\mathrm{T} + 3.421\mathrm{T}\exp\left[-\left(\mathrm{T}/125.1\right)^2\right] , \qquad (6.10)$$

in which T must be in kelvins. Murphy and Koop use (6.10), for example, to derive their expression for the saturation vapor pressure over ice, (4.4) above.

Figure 2 compares values for the specific heats of air, pure water, ice, and water vapor for temperatures between –40° and 40°C.

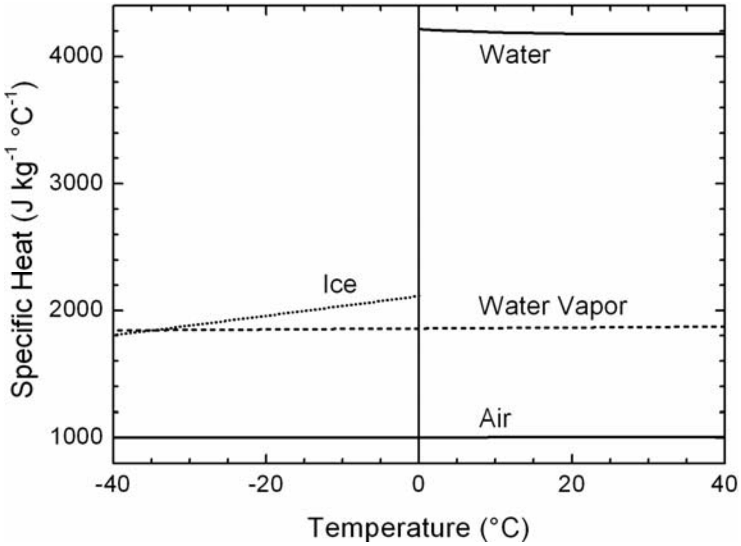

Figure 2. Specific heats at constant pressure of dry air [from (6.1)], water vapor [from (6.2)], pure water [from (6.9)], and pure ice [from (6.10)]. Notice, because the vertical axis has such a large range, the small variations in c_{pd}, c_{pv}, and c_{pw} are not obvious.

7 LATENT HEAT

Fleagle and Businger (1980, p. 113) give the following equations for the latent heats associated with the phase transitions of water molecules:

Latent heat of vaporization,

$$L_v = (25.00 - 0.02274T) \times 10^5 \; ; \tag{7.1}$$

Latent heat of fusion,

$$L_f = 3.34 \times 10^5 \; ; \tag{7.2}$$

Latent heat of sublimation,

$$L_s = (28.34 - 0.00149T) \times 10^5 \; . \tag{7.3}$$

Each of these gives the latent heat in J kg^{-1} when the temperature T is in °C.

The value for L_f in (7.2) is appropriate only near 0°C because L_f decreases with decreasing temperatures. Hobbs's (1974, p. 361) tabulation of L_f for temperatures below 0°C disagrees dramatically with a similar tabulation in the Smithsonian Meteorological Tables (List 1984, p. 343), however. The functions for L_v and L_s, on the other hand, agree quite well with the Smithsonian tabulation. The L_v values predicted by (7.1) are within 0.3% of the Smithsonian values for temperatures from 0° to 60°C, and the L_s values from (7.3) are within 0.2% of the Smithsonian values for temperatures between −50° and 0°C.

8 SURFACE TENSION OF WATER

Vargaftik et al. (1983) tabulate consensus values for the surface tension of pure water for temperatures between 0°C and the critical temperature, 374°C (Bohren and Albrecht 1998, p. 207ff.). They also develop from these data the following relation for computing the surface tension of pure water:

$$\sigma_w = 0.2358\left(\frac{374.00-T}{647.15}\right)^{1.256}\left[1-0.625\left(\frac{374.00-T}{647.15}\right)\right] . \qquad (8.1)$$

This gives σ_w in J m^{-2} when the water temperature T is in °C. This equation predicts exactly the values of surface tension that Lide (2001, p. 6-3) tabulates and matches the values in Batchelor (1970, p. 597) to within about 0.1%.

For temperatures between –45° and 0°C, Pruppacher and Klett (1997, p. 130) suggest computing the surface tension of pure water from

$$\begin{aligned}\sigma_w = {} & 7.593\times10^{-2} + 1.15\times10^{-4}\,T + 6.818\times10^{-5}\,T^2 + 6.511\times10^{-6}\,T^3 \\ & + 2.933\times10^{-7}\,T^4 + 6.283\times10^{-9}\,T^5 + 5.285\times10^{-11}\,T^6\end{aligned} , \qquad (8.2)$$

which again gives σ_w in J m^{-2} for T in °C. Unfortunately, (8.1) and (8.2) do not meet at 0°C. Equation (8.1) predicts 7.656×10^{-2} J m^{-2} there, while (8.2) gives 7.593×10^{-2} J m^{-2}. The former value is probably the more accurate one.

Pruppacher and Klett (1978, p. 107) likewise give an expression for the surface tension of an interface between water vapor and saline water. That expression, however, quantifies the salinity in terms of m_s/m_w, where m_w is the mass of pure water per unit volume and m_s is the mass of dissolved salt in the volume. Since the definition of salinity is

$$s = \frac{m_s}{m_w + m_s} , \qquad (8.3)$$

we see that

$$\frac{m_s}{m_w} = \frac{s}{1-s} , \qquad (8.4)$$

where s is the fractional salinity [s = S(in psu)/1000].

Hence, I convert Pruppacher and Klett's (1978) expression for the surface tension at a seawater interface to

$$\sigma_{sw} = \sigma_w + 2.77\times10^{-2}\left(\frac{s}{1-s}\right), \tag{8.5}$$

where σ_w comes from (8.1) or (8.2), depending on the water temperature. The coefficient multiplying the salinity term in (8.5) is virtually the same value that Hänel (1976) recommends. Equation (8.5) should be accurate for temperatures in [–25°, 40°C] and S in [0, 260 psu].

9 MEAN FREE PATHS OF AIR AND WATER VAPOR MOLECULES

The mean free path of a gas molecule is an estimate of the distance it travels between collisions with other molecules in the gas. Starting with equations that Wagner [1982, Eqs. (5.55), (5.56)] gives, I derive these expressions for the mean free paths of air molecules (λ_a) and water vapor molecules (λ_v) in air:

$$\lambda_a = \frac{kT}{\sqrt{2}\,\pi(P-e)d_a^2} , \tag{9.1}$$

$$\lambda_v = \frac{4kT}{\sqrt{1.622}\,\pi(P-e)(d_a+d_w)^2} , \tag{9.2}$$

where k = Boltzmann constant

T = temperature (K)

P = barometric pressure (Pa)

e = water vapor pressure (Pa)

d_a = diameter of an air molecule

d_w = diameter of a water molecule.

Equation (9.1) is essentially the same as Reif's (1967) expression for the mean free path of air molecules,

$$\lambda_a = \frac{kT}{\sqrt{2}\,\pi P d_a^2} . \tag{9.3}$$

In (9.1) and (9.2), λ_a and λ_v quantify the distance between consecutive collisions, not the distance between collisions between molecules of the same species. That is, a water vapor molecule will likely hit an air molecule next; λ_v estimates the distance from the previous to this next collision.

Using values for d_a and d_w of 3.7×10^{-10} m and 1.65×10^{-10} m, respectively[*], and expressing P and e in millibars, I simplify (9.1) and (9.2) to

---

[*] Personal communication, James H. Cragin, CRREL, 2000.

$$\lambda_a = \frac{2.3\times10^{-7}\,T}{P-e} \ , \tag{9.4}$$

$$\lambda_v = \frac{4.8\times10^{-7}\,T}{P-e} \ . \tag{9.5}$$

In these, λ_a and λ_v are in meters when T is in kelvins and P and e are in millibars.

For example, when T = 293 K and P – e = 1000 mb,

$$\lambda_a = 6.7\times10^{-8}\ \mathrm{m} \ , \tag{9.6}$$

$$\lambda_v = 1.4\times10^{-7}\ \mathrm{m} \ . \tag{9.7}$$

For comparison, Pruppacher and Klett (1978, p. 323) state without proof that $\lambda_a = 6.6 \times 10^{-8}$ m for $P = P_0$ and T = 293.15 K. Bohren and Albrecht (1998, p. 68) estimate $\lambda_a = 10^{-7}$ m for pressures near one atmosphere.

10 MOLECULAR VISCOSITY

10.1 Air

Hilsenrath et al. (1960, p. 10) give the following expression for the dynamic viscosity of air:

$$\eta_a = \frac{1.458\times10^{-6}\,T^{3/2}}{T + 110.4} \ . \tag{10.1}$$

Here, η_a is in kg m^{-1} s^{-1} when T is in kelvins, and they suggest that this relation is accurate for a pressure of one atmosphere for temperatures between 100 and 1900 K.

The kinematic viscosity of air, ν_a, however, occurs more commonly in boundary-layer studies. We can obtain this from η_a as

$$\nu_a \equiv \frac{\eta_a}{\rho_d} \ . \tag{10.2}$$

I have combined this definition, (2.2), and (10.1) to obtain a polynomial expression for predicting ν_a for the temperature range [–50°, 50°C];

$$\nu_a = 1.326\times10^{-5}\left(1 + 6.542\times10^{-3}\,T + 8.301\times10^{-6}\,T^2 - 4.840\times10^{-9}\,T^3\right). \tag{10.3}$$

Here, ν_a is in m^2 s^{-1}, and T is in °C.

Figure 3 shows (10.3) plotted as a function of temperature; Table 4 lists these values. The predictions from (10.3) agree to three significant figures with values tabulated in Goldstein (1965, p. 7) and Batchelor (1970, p. 594).

10.2 Water

Reid et al. (1987, p. 441, 455) give the following expression for the dynamic viscosity of pure water:

$$\eta_w = 10^{-3}\exp\left(-24.71 + 4.209\times10^{3}\,T^{-1} + 4.527\times10^{-2}\,T - 3.376\times10^{-5}\,T^2\right). \tag{10.4}$$

As with (10.1), here η_w is in kg m^{-1} s^{-1}, and the temperature is in kelvins.

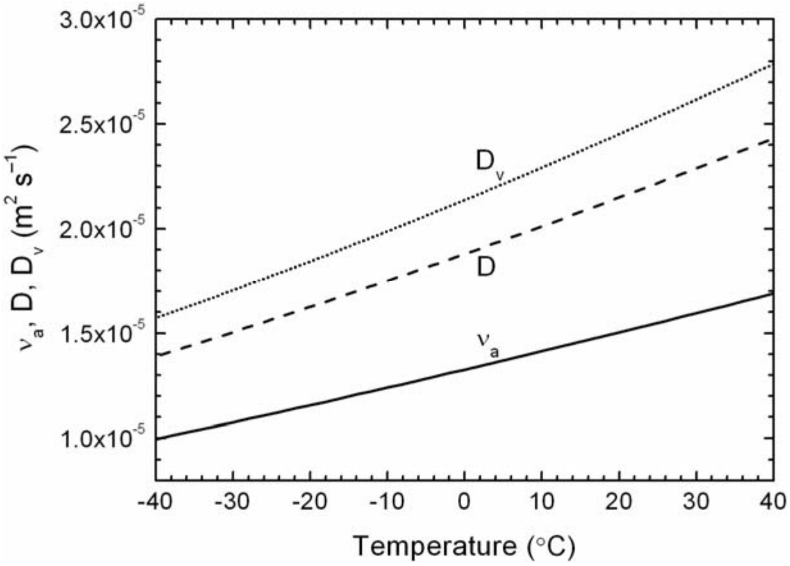

Figure 3. Molecular values of the kinematic viscosity (ν_a) and thermal diffusivity (D) of air and of the water vapor diffusivity (D_v) in air at a barometric pressure of 1000 mb. The calculations of viscosity and thermal diffusivity assume dry air.

Because Neumann and Pierson (1966, p. 52) suggest that salinity and pressure affect the dynamic viscosity of water only slightly, I compute the kinematic viscosity of pure water (ν_w) and seawater (ν_{sw}) from

$$\nu_w = \frac{\eta_w}{\rho_w} \qquad (10.5)$$

and

$$\nu_{sw} = \frac{\eta_w}{\rho_{sw}} \ . \qquad (10.6)$$

In these, ν_w and ν_{sw} are in $m^2\ s^{-1}$; and ρ_w and ρ_{sw} come from (5.1) and (5.2), respectively.

As examples of these calculations, for T = 20°C, S = 34 psu, and pressures near one atmosphere, I find $\eta_w = 1.018 \times 10^{-3}$ kg m^{-1} s^{-1}, $\rho_w = 998.2$ kg m^{-3}, $\rho_{sw} = 1024.0$ kg m^{-3}, $\nu_w = 1.019 \times 10^{-6}$ m^2 s^{-1}, and $\nu_{sw} = 0.994 \times 10^{-6}$ m^2 s^{-1}. In particular, these η_w and ν_w values and values I have calculated at other temperatures are within 3% of values tabulated in Horne (1969, p. 486) and Batchelor (1970, p. 597).

Table 4. Molecular values of the kinematic viscosity (ν_a) and thermal diffusivity (D) of air, the diffusivity of water vapor in air (D_v), and the Prandtl (Pr) and Schmidt (Sc) numbers. Calculations of the thermal diffusivity assume dry air. The barometric pressure is assumed to be 1000 mb.

Temperature (°C)	$10^5\ \nu_a$ ($m^2\ s^{-1}$)	10^5 D ($m^2\ s^{-1}$)	$10^5\ D_v$ ($m^2\ s^{-1}$)	Pr	Sc
–40	0.997	1.389	1.573	0.718	0.634
–35	1.036	1.446	1.639	0.716	0.632
–30	1.076	1.505	1.706	0.715	0.631
–25	1.116	1.565	1.775	0.713	0.629
–20	1.157	1.626	1.845	0.711	0.627
–15	1.198	1.688	1.916	0.710	0.625
–10	1.240	1.751	1.989	0.708	0.624
–5	1.283	1.815	2.063	0.707	0.622
0	1.326	1.880	2.138	0.705	0.620
5	1.370	1.946	2.215	0.704	0.618
10	1.414	2.012	2.292	0.703	0.617
15	1.459	2.080	2.372	0.701	0.615
20	1.504	2.149	2.452	0.700	0.613
25	1.550	2.218	2.534	0.699	0.612
30	1.596	2.289	2.617	0.697	0.610
35	1.643	2.360	2.701	0.696	0.608
40	1.690	2.432	2.787	0.695	0.606

11 THERMAL CONDUCTIVITY AND THERMAL DIFFUSIVITY OF AIR

Hilsenrath et al. (1960, p. 70) also tabulate the thermal conductivity of air, k_a. I have fitted their data for temperatures between –193° and 277°C with the following polynomial:

$$k_a = 2.411\times10^{-2}\left(1 + 3.309\times10^{-3}\,T - 1.441\times10^{-6}\,T^2\right) . \qquad (11.1)$$

This gives k_a in W m^{-1} $°C^{-1}$ for temperature T in °C.

The thermal diffusivity D is analogous as a molecular transport variable to the kinematic viscosity ν_a. We define D as

$$D = \frac{k_a}{\rho_d\, c_p} , \qquad (11.2)$$

which has units of m^2 s^{-1}. Figure 3 plots D as a function of temperature, while Table 4 lists values for normal atmospheric boundary layer temperatures.

Notice that, in general, ρ_a and c_p in (11.2) should include the effects of atmospheric water vapor. I have ignored those small effects in creating Figure 3 and Table 4 because (11.1) predicts the thermal conductivity of dry air. I presume that including water vapor effects in k_a would tend to offset the effects of water vapor in ρ_a and c_p and would, thus, yield a thermal conductivity D comparable to the dry-air value that I have calculated.

12 MOLECULAR DIFFUSIVITIES OF GASES IN AIR

12.1 Water Vapor

Hall and Pruppacher (1976) developed the following expression for the molecular diffusivity of water vapor in air:

$$D_v = 2.11\times10^{-5}\left(\frac{T}{T_0}\right)^{1.94}\left(\frac{P_0}{P}\right) . \qquad (12.1)$$

This gives D_v in $m^2\ s^{-1}$ for temperature T in kelvins and pressure P in millibars. Hall and Pruppacher explain that no good measurements of D_v exist for temperatures below 0°C. Therefore, they obtain (12.1) by extrapolating measurements above freezing to subfreezing temperatures. Still, Hall and Pruppacher claim that (12.1) applies over the temperature interval [–80°, 40°C]. Pruppacher and Klett (1978, p. 413) originally recommended (12.1), and Pruppacher and Klett (1997, p. 503) still do. Figure 3 and Table 4 compare values of D_v with ν_a and D.

The Prandtl (Pr) and Schmidt (Sc) numbers compare the relative efficiencies of molecular exchange processes. The molecular Prandtl number for air is

$$\mathrm{Pr} \equiv \frac{\nu_a}{D} , \qquad (12.2)$$

and the molecular Schmidt number for air is

$$\mathrm{Sc} \equiv \frac{\nu_a}{D_v} . \qquad (12.3)$$

We can compute these from (10.3), (11.2), and (12.1). Table 4 also lists values of Pr and Sc for P = 1000 mb and temperatures in the range [–40°, 40°C].

12.2 Other Atmospheric Gases

The molecular diffusivities of atmospheric trace gases such as carbon dioxide, methane, and nitrous oxide also occur in atmospheric boundary layer research. Reid et al. (1987, p. 587) give a semi-empirical expression, which they adapted from Fuller et al. (1969), to predict how the diffusivities of these trace atmospheric gases depend on temperature and pressure.

Table 5 lists diffusivities in air for several environmentally important gases. I have computed some of these (labeled "D_{g0}, Reid et al.") for $T_0 = 273.15$ K and $P_0 = 1013.25$ mb from equation (11-4.4) and Table 11.1 in Reid et al. (1987). For comparison, I also include in Table 5 diffusivity values (labeled D_{gT}) at temperatures of 0°C (273.15 K) or 25°C (298.15 K) that Thibodeaux (1979, 1996) tabulates. Thibodeaux, however, does not mention the barometric pressure corresponding to his values; I therefore assume it is approximately one atmosphere.

Equation (11-4.4) in Reid et al. (1987) implies a general expression for how the diffusivities of gases in air depend on temperature and pressure,

$$D_g = D_{g0}\left(\frac{T}{T_0}\right)^{1.75}\left(\frac{P_0}{P}\right) . \tag{12.4}$$

In this, D_g is in $m^2\ s^{-1}$, T is in kelvins, P is in millibars, and D_{g0} is the value at T_0 and P_0 in Table 5. Alternatively, we could just as well substitute Thibodeaux's (1979, 1996) values for D_{gT} in place of D_{g0} in (12.4), replace T_0 with the tabulated temperature, and assume that Thibodeaux's listed values all correspond to pressure P_0.

Massman (1998) also reviews the diffusivities of various gases in air in the context of an equation like (12.4) but assumes that the exponent is 1.81:

$$D_g = D_{g0}\left(\frac{T}{T_0}\right)^{1.81}\left(\frac{P_0}{P}\right) . \tag{12.5}$$

Table 5 lists the values that he recommends for D_{g0}. Coincidently, the Smithsonian Meteorological Tables (List 1984, p. 395) also suggests a relation like (12.5) for the diffusivities of gases in air.

Comparing the D_{gT} values reported at 273.15 K directly with the D_{g0} values in Table 5 or using (12.4) or (12.5) to convert the Reid et al. (1987), Massman (1998), or Thibodeaux (1979, 1996) values to the same temperature lets us evaluate the uncertainty in these gas diffusivities.

For example, the four diffusivities listed in Table 5 for carbon dioxide have a spread of only $0.06 \times 10^{-5}\ m^2\ s^{-1}$ at 0°C. The diffusivities for ammonia, on the other hand, have a spread of about $0.5 \times 10^{-5}\ m^2\ s^{-1}$ at 0°C.

Table 5 also includes four new estimates of the water vapor diffusivity to compare with (12.1). The two values from Thibodeaux (1979, 1996) both predict

Table 5. Molecular diffusivities of various gases in air. The columns labeled D_{g0} show predictions based on equation (11-4.4) and Table 11.1 in Reid et al. (1987) and recommendations by Massman (1998). These values are appropriate at temperature T_0 = 273.15 K and pressure P_0 = 1013.25 mb. The D_{gT} column shows values tabulated in Thibodeaux (1979, Table C.8, superscript 1) or Thibodeaux (1996, Table C.6, superscript 2) for the temperatures indicated.

	10^5 D_{g0} (m^2 s^{-1})			
Gas	**Reid et al.**	**Massman**	**Temperature (K)**	**10^5 D_{gT} (m^2 s^{-1})**
Ammonia, NH_3	1.88	1.98	273.15	2.16[1]
			298.15	2.8[2]
Bromine, Br^2	0.971		298.15	1.00[2]
Carbon dioxide, CO_2	1.35	1.38	273.15	1.38[1]
			298.15	1.64[2]
Carbon monoxide, CO	1.71	1.81	298.15	2.03[2]
Hydrogen sulfide, HS			298.15	1.66[2]
Methane, CH_4		1.95	273.15	1.6[2]
Nitrogen dioxide, NO_2		1.36		
Nitric oxide, NO		1.80	298.15	2.04[2]
Nitrous oxide, N_2O	1.22	1.44	298.15	1.55[2]
Ozone, O_3		1.44		
Sulfur hexafluoride, SF_6	0.795			
Sulfur dioxide, SO_2	1.08	1.09	273.15	1.03[2]
Water vapor, H_2O	2.15	2.18	273.15	2.20[1]
			298.15	2.56[2]

$D_v = 2.20 \times 10^{-5}$ m^2 s^{-1} at 0°C. The comparable value that I predict from Reid et al. (1987) is $D_v = 2.15 \times 10^{-5}$ m^2 s^{-1}, while Massman (1998) recommends $D_v = 2.18 \times 10^{-5}$ m^2 s^{-1}. Hall and Pruppacher's (1976) equation, (12.1), gives $D_v = 2.11 \times 10^{-5}$ m^2 s^{-1} at 0°C and 1013.25 mb. Consequently, I conclude that the diffusivities for the gases listed in Table 5 are typically known to an accuracy of ±3%. Massman similarly concludes that most of the diffusivities listed in Table 5 have an absolute uncertainty that is no more than 5–9%, though the tabulated diffusivities for O_3, NO, and NO_2 might be uncertain by 25% because of the paucity of data for these molecules.

13 EFFECTS OF SURFACE CURVATURE ON k_a AND D_V

The transfers of heat and moisture at the surface of small atmospheric particles, like cloud droplets, sea spray droplets, snowflakes, and aerosols, cannot strictly be parameterized in terms of the k_a and D_v values given above. Because of the extreme curvature of the surface of these small particles, the air around them no longer behaves as a continuum. This is the so-called Kelvin effect (e.g., Pruppacher and Klett 1997, p. 170). Likewise, surface curvature will also affect the transfers of heat and moisture around the snow grains in a snowpack, which is always porous.

Pruppacher and Klett (1997) present equations to account for how these curvature effects modify k_a and D_v (also Andreas 1989, 1990, 1995). For predicting the effects of curvature on k_a, they give (Pruppacher and Klett 1997, p. 509)

$$k_a' = \frac{k_a}{\dfrac{r_0}{r_0 + \Delta_T} + \dfrac{k_a}{r_0\,\alpha_T\,\rho_a\,c_p}\left(\dfrac{2\pi M_a}{RT}\right)^{1/2}} , \qquad (13.1)$$

where k_a' = thermal conductivity modified for curvature effects (W m^{-1} K^{-1})

r_0 = particle radius (m)

Δ_T = empirical constant (= 2.16×10^{-7} m)

α_T = empirical constant (= 0.7)

T = temperature (K).

In (13.1), we recognize $k_a/\rho_a c_p$ from (11.2) as the thermal diffusivity D. Hence, if we divide (13.1) by $\rho_a c_p$, we get an analogous expression for curvature effects on the thermal diffusivity,

$$D' = \frac{D}{\dfrac{r_0}{r_0 + \Delta_T} + \dfrac{D}{r_0\,\alpha_T}\left(\dfrac{2\pi M_a}{RT}\right)^{1/2}} . \qquad (13.2)$$

This predicts the modified thermal diffusivity in m^2 s^{-1}.

Similarly, Pruppacher and Klett (1997, p. 506) give the following equation for predicting how surface curvature influences the vapor diffusivity around small particles:

$$D_v' = \frac{D_v}{\dfrac{r_0}{r_0 + \Delta_v} + \dfrac{D_v}{r_0\,\alpha_c}\left(\dfrac{2\pi M_w}{R\,T}\right)^{1/2}} , \tag{13.3}$$

where D_v' = water vapor diffusivity modified for curvature effects ($m^2\ s^{-1}$)

α_c = empirical constant (= 0.036)

Δ_v = empirical constant (= $1.3\lambda_a = 8.7 \times 10^{-8}$ m for typical sea-level temperature and pressure).

Figure 4 compares k_a' with k_a and D_v' with D_v for particles with radii between 0.1 and 1000 μm, which is a typical size range for sea spray droplets (cf. Andreas 1989). According to this figure, curvature effects significantly influence sensible heat transfer only around particles with radii less than about 5 μm. In contrast, surface curvature significantly decreases the rate of vapor diffusion around particles with radii up to about 200 μm.

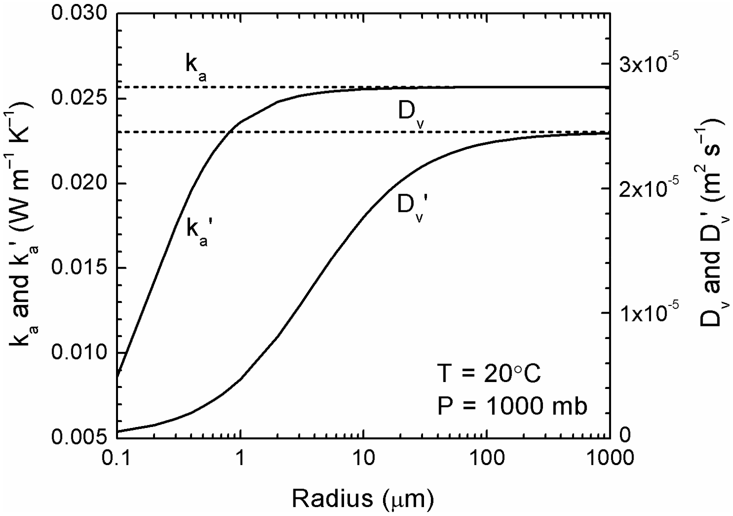

Figure 4. Effects of surface curvature on the thermal conductivity of air [k_a', from (13.1)] and on the water vapor diffusivity in air [D_v', from (13.3)]. The plot also shows for comparison the unmodified values, k_a [from (11.1)] and D_v [from (12.1)]. The air temperature is assumed to be 20°C, and the barometric pressure is 1000 mb.

14 WIND FORCE SCALES

14.1 Beaufort Scale

A common way to describe wind and sea state is with the Beaufort Scale. In the early nineteenth century, Admiral Sir Francis Beaufort developed a scale for wind force based on the behavior of sailing ships. The British Admiralty later adopted this scale, and Bowditch (1977, p. 1059) helped popularize it.

In effect, the Beaufort number or force B is related to the wind speed (in m s^{-1}) at a standard reference height of 10 m, U_{10}, through (List 1984, p. 119; Strangeways 2001)

$$U_{10} = 0.836 B^{3/2} \quad . \tag{14.1}$$

But the key feature of the Beaufort Scale is that it associates U_{10} and B with a description of wind and sea state and, thus, provides an estimate of U_{10} from visual observations alone.

Subsequently, the Beaufort Scale was adapted to use over land (e.g., Bowditch 1977, p. 1059; List 1984, p. 119). Table 6 shows the Beaufort Scale and includes descriptions of conditions for a given Beaufort force over both land and sea.

14.2 Saffir-Simpson Scale

The Beaufort Scale classifies all ocean storms with surface-level winds above 32.7 m s^{-1} as hurricanes. But conditions at sea and when the storm comes ashore vary widely depending on the wind speed. The Saffir-Simpson Scale, developed by Herbert Saffir and Bob Simpson, further divides hurricanes into five categories. Table 7 shows the Saffir-Simpson Scale.

At sea, storms are assigned to a Saffir-Simpson category on the basis of their maximum surface-level wind speed and minimum central pressure. Storms may change category during their lifetime as they intensify or degrade. The “Storm Surge” listed in Table 7 is the height of the ocean wave that comes ashore ahead of the storm. The values shown give a typical range; the actual storm surge will depend on the slope of the continental shelf.

The main relevance of the Saffir-Simpson Scale is that it attempts to forecast flooding and damage if the storm does move onshore. The “Effects” column in the table lists these predictions. Effects range from minor for a Category 1 storm to catastrophic, as they were with Mitch, a 1998 Category 5 hurricane that killed over 800 people in Honduras and Nicaragua.

Table 6. Beaufort Scale, with the associated wind speed ranges for each Beaufort force in meters per second, knots, and miles per hour. $H_{1/3}$ is the significant wave height, the average height of the highest one-third of all waves occurring during a period (Kinsman 1965, p. 302f, 390f.).

Force	Wind description	U_{10}			$H_{1/3}$ (m)	Over the sea	Over land
		(m s^{-1})	(knots)	(mph)			
0	Calm	0.0–0.2	<1	<1	0	Sea like a mirror	Calm; smoke rises vertically
1	Light air	0.3–1.5	1–3	1–3	0.1–0.2	Ripples with appearance of scales; no foam crests	Smoke drift indicates wind direction; vanes do not move
2	Light breeze	1.6–3.3	4–6	4–7	0.3–0.5	Small wavelets; crests have glassy appearance but do not break	Wind felt on face; leaves rustle; vanes begin to move
3	Gentle breeze	3.4–5.4	7–10	8–12	0.6–1.0	Large wavelets; crests begin to break; scattered whitecaps	Leaves and twigs in constant motion; light flags extended
4	Moderate breeze	5.5–7.9	11–16	13–18	1.5	Small waves becoming longer; numerous whitecaps	Dust, leaves, and loose paper raised; small branches move; flags flap
5	Fresh breeze	8.0–10.7	17–21	19–24	2.0	Moderate waves taking longer form; many whitecaps and chance of some spray	Small trees in leaf begin to sway; whitecaps on inland waters
6	Strong breeze	10.8–13.8	22–27	25–31	3.5	Large waves forming; white foam crests extensive, and spray probable	Larger branches of trees in motion; flags pop; whistling in wires; umbrellas unstable
7	Moderate gale	13.9–17.1	28–33	32–38	5.0	Sea heaps up, and white foam from breaking waves begins to be blown in streaks; spindrift appears	Whole trees in motion; resistance felt in walking against the wind
8	Fresh gale	17.2–20.7	34–40	39–46	7.5	Moderately high waves of greater length; edges of crests break into spindrift; foam is blown in well-marked streaks	Twigs and small branches broken; progress generally impeded
9	Strong gale	20.8–24.4	41–47	47–54	9.5	High waves; dense streaks of foam; sea begins to roll; spray may reduce visibility	Slight structural damage occurs; slate blown from roofs
10	Whole gale	24.5–28.4	48–55	55–63	12	Very high waves with overhanging crests; sea surface takes on white appearance as foam in great patches is blown in very dense streaks; rolling sea is heavy; visibility reduced	Seldom experienced on land; trees broken or uprooted; considerable structural damage occurs
11	Storm	28.5–32.6	56–63	64–72	15	Exceptionally high waves; sea covered with long white patches of foam; small and medium-sized ships might be lost to view behind waves; visibility further reduced	Very rarely experienced on land; usually accompanied by widespread damage
12	Hurricane	>32.7	>64	>73	>15	Air filled with foam and spray; sea completely white with driving spray; visibility greatly reduced	

Table 7. Saffir-Simpson Scale for hurricane intensity. The maximum sustained winds are given in meters per second, knots, and miles per hour.

Category	Sustained winds			Central pressure (mb)	Storm surge (m)	Effects
	($m\ s^{-1}$)	(knots)	(mph)			
Tropical storm	17–32	35–63	39–73			Beaufort force 8–11
1	33–42	64–82	74–95	>980	1.0–1.7	No real damage to buildings. Damage primarily to unanchored mobile homes, shrubbery, and trees. Some flooding of coastal roads and minor damage to piers.
2	43–49	83–95	96–110	979–965	1.8–2.6	Some damage to doors, windows, and roofing material. Considerable damage to vegetation, mobile homes, and piers. Coastal low-lying escape routes flood 2–4 hours before the storm center arrives. Small craft in unprotected anchorages break moorings.
3	50–58	96–113	111–130	964–945	2.7–3.8	Some structural damage to small residences and utility buildings, with a minor amount of curtainwall failures. Mobile homes are destroyed. Flooding near the coast destroys smaller structures, with larger structures damaged by floating debris. Terrain continuously lower than 5 feet above sea level may be flooded 8 miles or more inland.
4	59–69	114–135	131–155	944–920	3.9–5.6	More extensive curtainwall failures, with some roofs on small residences failing completely. Major beach erosion. Major damage to the lower floors of structures near the shore. Terrain continuously lower than 10 feet above sea level may be flooded inland as far as 6 miles; massive evacuation of residential areas could, therefore, be required.
5	>69	>135	>155	<920	>5.7	Complete roof failure on many residences and industrial buildings. Some complete building failures, with small utility buildings blown over or away. Major damage to lower floors of all structures located less than 15 feet above sea level and within 500 yards of the shore. Massive evacuation may be required for residential areas on low ground within 5 to 10 miles of the shore.

14.3 Fujita Scale

Similarly, the Fujita Scale categorizes tornadoes in terms of their maximum wind speed and the damage they cause (Fujita 1981; Glickman 2000, p. 322f.). Table 8 shows the Fujita Scale. Fujita (1981) associated the lower surface-level wind speed limit for a tornado category with the Fujita number F through the expression

$$U = 6.30\left(F + 2\right)^{3/2} , \qquad (14.2)$$

where U is the wind speed in m s^{-1}.

Table 8. Fujita Scale to describe tornado intensity. The range for maximum wind speeds is given in meters per second and miles per hour.

Fujita scale	Wind speed range		Damage specifications
	(m s^{-1})	(mph)	
F0	18–32	40–72	Beaufort force 8–11. Light damage. Some damage to chimneys; branches break off trees; some shallow-rooted trees pushed over; damage to sign boards.
F1	33–49	73–112	Moderate damage. The lower wind speed is the beginning of the hurricane range. Surfaces of roofs peeled off; mobile homes pushed off foundations or overturned; moving autos pushed off the road.
F2	50–69	113–157	Considerable damage. Roofs torn off frame houses; mobile homes demolished; boxcars pushed over; large trees snapped off or uprooted; light-object missiles generated.
F3	70–92	158–206	Severe damage. Roofs and some walls torn off well-constructed houses; trains overturned; most trees in a forest uprooted; heavy cars lifted off the ground and thrown.
F4	93–116	207–260	Devastating damage. Well-constructed houses leveled; structures with weak foundations blown off some distance; cars thrown; large missiles generated.
F5	117–142	261–318	Incredible damage. Strong frame houses lifted off foundations and carried considerable distance to disintegrate; automobile-sized missiles fly through the air in excess of 100 m; bark ripped from trees; incredible phenomena occur.
F6+	>142	>318	Tornadoes are not expected to reach F6 wind speeds.

15 CONCLUSIONS

For the functions that I have presented that are based on fits to data, I have generally tried to estimate the uncertainty in the predicted values. In preparing this review, however, I was surprised to see how old some of the data are that constitute the bases for these fits. For example, Hilsenrath et al. (1960), from which I take several functions, was published more than 40 years ago. Likewise, although my copy of the Smithsonian Meteorological Tables (List 1984) has a 1984 publication date, this volume is essentially just a reprinting of the original 1951 tables. Although I have no reason to doubt the quality of these older data, repeating measurement of some of these important thermophysical quantities with modern instruments should reduce the uncertainties that I have identified.

In particular, many of the gas diffusivities listed in Table 5 are based on just theory or only a few measurements. The gases in this table—and others for which I could find no information—are environmentally important for several reasons: Some are greenhouse gases, some are pollutants, and others are useful as environmental tracers. Hence, better data on their behaviors in air is crucial. For example, the data are generally so scanty that we still cannot decide how to predict the temperature dependence of the diffusivity, as reflected in the variety of exponents in (12.1), (12.4), and (12.5). In my view, measuring these diffusivities over a range of temperatures and pressures is vital research.

REFERENCES

Andreas, E.L (1989) Thermal and size evolution of sea spray droplets. CRREL Report 89-11, U.S. Army Cold Regions Research and Engineering Laboratory, Hanover, New Hampshire, 37 p. (NTIS: AD A210484.)

Andreas, E.L (1990) Time constants for the evolution of sea spray droplets. *Tellus*, **42B**: 481–497.

Andreas, E.L (1995) The temperature of evaporating sea spray droplets. *Journal of the Atmospheric Sciences*, **52**: 852–862.

Batchelor, G.K. (1970) *An Introduction to Fluid Dynamics*. Cambridge, U.K.: Cambridge University Press, 615 p.

Bohren, C.F., and B.A. Albrecht (1998) *Atmospheric Thermodynamics*. New York: Oxford University Press, 402 p.

Bowditch, N. (1977) *American Practical Navigator, Vol. 1*. Publication No. 9, Washington, D.C.: Defense Mapping Agency Hydrographic Center, 1386 p.

Brock, F.V., and S.J. Richardson (2001) *Meteorological Measurement Systems*. New York: Oxford University Press, 290 p.

Bromley, L.A., V.A. Desaussure, J.C. Clipp, and J.S. Wright (1967) Heat capacities of sea water solutions at salinities of 1 to 12% and temperatures of 2° to 80°C. *Journal of Chemical and Engineering Data*, **12**: 202–206.

Buck, A.L. (1981) New equations for computing vapor pressure and enhancement factor. *Journal of Applied Meteorology*, **20**: 1527–1532.

Businger, J.A. (1982) The fluxes of specific enthalpy, sensible heat and latent heat near the Earth's surface. *Journal of the Atmospheric Sciences*, **39**: 1889–1892.

Cox, R.A., and N.D. Smith (1959) The specific heat of sea water. *Proceedings of the Royal Society, London,* **A252**: 51–62.

Fleagle, R.G., and J.A. Businger (1980) *An Introduction to Atmospheric Physics*. 2nd ed. New York: Academic Press, 432 p.

Fuehrer, P.L., and C.A. Friehe (2002) Flux corrections revisited. *Boundary-Layer Meteorology*, **102**: 415–457.

Fujita, T.T. (1981) Tornadoes and downbursts in the context of generalized planetary scales. *Journal of the Atmospheric Sciences*, **38**: 1511–1534.

Fuller, E.N., K. Ensley, and J.C. Giddings (1969) Diffusion of halogenated hydrocarbons in helium. The effect of structure on collision cross section. *Journal of Physical Chemistry*, **73**: 3679–3685.

Gill, A.E. (1982) *Atmosphere-Ocean Dynamics*. New York: Academic Press, 662 p.

Glickman, T.S. (Ed.) (2000) *Glossary of Meteorology*. 2nd ed. Boston: American Meteorological Society, 855 p.

Goldstein, S. (Ed.) (1965) *Modern Developments in Fluid Dynamics, Vol. 1*. New York: Dover, 330 p.

Hall, W.D., and H.R. Pruppacher (1976) The survival of ice particles falling from cirrus clouds in subsaturated air. *Journal of the Atmospheric Sciences*, **33**: 1995–2006.

Hänel, G. (1976) The properties of atmospheric aerosol particles as functions of the relative humidity at thermodynamic equilibrium with the surrounding moist air. *Advances in Geophysics*, **19**, New York: Academic Press, 73–188.

Hare, D.E., and C.M. Sorensen (1987) The density of supercooled water. II. Bulk samples cooled to the homogeneous nucleation limit. *Journal of Chemical Physics*, **87**: 4840–4845.

Hilsenrath, J., C.W. Beckett, W.S. Benedict, L. Fano, H.J. Hoge, J.F. Masi, R.L. Nuttall, Y.S. Touloukian, and H.W. Woolley (1960) *Tables of Thermodynamic Transport Properties of Air, Argon, Carbon Dioxide, Carbon Monoxide, Hydrogen, Nitrogen, Oxygen, and Steam*. Oxford, U.K.: Pergamon Press, 478 p.

Hobbs, P.V. (1974) *Ice Physics*. Oxford, U.K.: Clarendon Press, 837 p.

Horne, R.A. (1969) *Marine Chemistry*. New York: Wiley-Interscience, 568 p.

Iribarne, J.V., and W.L. Godson (1981) *Atmospheric Thermodynamics*. 2nd ed. Dordrecht: D. Reidel, 259 p.

Kester, D.R. (1974) Comparison of recent seawater freezing point data. *Journal of Geophysical Research*, **79**: 4555–4556.

Kinsman, B. (1965) *Wind Waves*. Englewood Cliffs, New Jersey: Prentice-Hall, 676 p.

Larsen, S.E., and N.E. Busch (1974) Hot-wire measurements in the atmosphere: Part 1. Calibration and response characteristics. *DISA Information*, **16**: 15–34.

Lide, D.R. (Ed.) (2001) *CRC Handbook of Chemistry and Physics*. 82nd ed. Boca Raton, Florida: CRC Press.

List, R.J. (1984) *Smithsonian Meteorological Tables*. Sixth ed. Washington, D.C.: Smithsonian Institution Press, 527 p.

Lumley, J.L., and H.A. Panofsky (1964) *The Structure of Atmospheric Turbulence*. New York: Wiley-Interscience, 239 p.

Massman, W.J. (1998) A review of the molecular diffusivities of H_2O, CO_2, CH_4, CO, O_3, SO_2, NH_3, N_2O, NO, and NO_2 in air, O_2, and N_2 near STP. *Atmospheric Environment*, **32**: 1111–1127.

Millero, F.J., G. Perron, and J.E. Desnoyes (1973) Heat capacity of seawater solutions from 5° to 35°C and 0.5 to 22‰ chlorinity. *Journal of Geophysical Research*, **78**: 4499–4507.

Murphy, D.M., and T. Koop (2005) Review of the vapour pressures of ice and supercooled water for atmospheric applications. *Quarterly Journal of the Royal Meteorological Society*, **131**: 1539–1565.

Neumann, G., and W.J. Pierson, Jr. (1966) *Principles of Physical Oceanography*. Englewood Cliffs, N.J.: Prentice-Hall, 545 p.

Pruppacher, H.R., and J.D. Klett (1978) *Microphysics of Clouds and Precipitation*. Dordrecht: D. Reidel, 714 p.

Pruppacher, H.R., and J.D. Klett (1997) *Microphysics of Clouds and Precipitation*. 2nd revised ed. Dordrecht: Kluwer, 954 p.

Reid, R.C., J.M. Prausnitz, and B.E. Poling (1987) *The Properties of Gases and Liquids*. 4th ed. New York: McGraw-Hill, 741 p.

Reif, F. (1967) *Statistical Physics: Berkeley Physics Course*, *Vol. 5*. New York: McGraw-Hill, 398 p.

Roll, H.U. (1965) *Physics of the Marine Atmosphere*. New York: Academic Press, 426 p.

Schwerdtfeger, P. (1976) *Physical Principles of Micro-Meteorological Measurements*. Amsterdam: Elsevier, 113 p.

Strangeways, I. (2001) Back to basics: The ‘met enclosure:’ Part 6–Wind. *Weather*, **56**: 154–161.

Thibodeaux, L.J. (1979) *Chemodynamics: Environmental Movement of Chemicals in Air, Water, and Soil*. New York: Wiley-Interscience, 501 p.

Thibodeaux, L.J. (1996) *Environmental Chemodynamics: Movement of Chemicals in Air, Water, and Soil*. 2nd ed. New York: John Wiley and Sons, 593 p.

Vargaftik, N.B., B.N. Volkov, and L.D. Voljak (1983) International tables of the surface tension of water. *Journal of Physical and Chemical Reference Data*, **12**: 817–820.

Wagner, P.E. (1982) Aerosol growth by condensation. *Aerosol Microphysics II: Chemical Physics of Microparticles* (W.H. Marlow, ed.). Berlin: Springer-Verlag, 129–178.

REPORT DOCUMENTATION PAGE

Form Approved
OMB No. 0704-0188

1. REPORT DATE *(DD-MM-YYYY)*
October 2005

2. REPORT TYPE
Monograph

3. DATES COVERED *(From - To)*

4. TITLE AND SUBTITLE
Handbook of Physical Constants and Functions for Use in
Atmospheric Boundary Layer Studies

5a. CONTRACT NUMBER

5b. GRANT NUMBER

5c. PROGRAM ELEMENT NUMBER

6. AUTHOR(S)
Edgar L Andreas

5d. PROJECT NUMBER

5e. TASK NUMBER

5f. WORK UNIT NUMBER

7. PERFORMING ORGANIZATION NAME(S) AND ADDRESS(ES)

U.S. Army Engineer Research and Development Center
Cold Regions Research and Engineering Laboratory
72 Lyme Road
Hanover, NH. 03755-1290

8. PERFORMING ORGANIZATION REPORT NUMBER

ERDC/CRREL M-05-1

9. SPONSORING / MONITORING AGENCY NAME(S) AND ADDRESS(ES)
Department of the Army

Office of Naval Research

10. SPONSOR/MONITOR'S ACRONYM(S)

11. SPONSOR/MONITOR'S REPORT NUMBER(S)

12. DISTRIBUTION / AVAILABILITY STATEMENT
Approved for public release; distribution is unlimited

Available from NTIS, Springfield, Virginia 22161

13. SUPPLEMENTARY NOTES

14. ABSTRACT
Studies of the atmospheric boundary layer always require values for the dynamic and thermodynamic properties of the fluids present: namely, air, water vapor, and other trace gases. Studies of the marine boundary layer frequently require similar properties for the ocean, in addition. This handbook collects functions for calculating the values for these dynamic and thermodynamic variables. For example, it includes equations for air density, water vapor density, and seawater density. It also describes various humidity variables and shows how to convert among these. It includes equations for the specific heats of dry air, water vapor, moist air, seawater, and ice and for the latent heats of water in its various phases. The handbook goes on to show how to calculate the molecular transport properties such as the thermal conductivity of air and the diffusivities of heat, water vapor, and several environmentally important gases in air. This discussion naturally includes values for the molecular Prandtl and Schmidt numbers. Finally, the handbook concludes with summaries of several wind force scales that descriptively categorize winds on land and sea: the Beaufort Scale, the Saffir-Simpson Scale for hurricanes, and the Fujita Scale for tornadoes.

15. SUBJECT TERMS
Air density
Beaufort Scale
Diffusivities in air
Fujita Scale
Latent heat
Mean free path
Saffir-Simpson Scale
Specific heat
Surface tension of water
Thermal conductivity of air
Viscosity
Water density
Water vapor variables

16. SECURITY CLASSIFICATION OF:			**17. LIMITATION OF ABSTRACT**	**18. NUMBER OF PAGES**	**19a. NAME OF RESPONSIBLE PERSON**
a. REPORT	**b. ABSTRACT**	**c. THIS PAGE**			**19b. TELEPHONE NUMBER** *(include area code)*
U	U	U	U	52	

Standard Form 298 (Rev. 8-98)
Prescribed by ANSI Std. 239.18